Improvement of oncolytic adenovirus vectors through genetic capsid modifications

Vrij, J. de

CHAPTER 5

A CATHEPSIN-CLEAVAGE SITE BETWEEN THE ADENOVIRUS CAPSID PROTEIN IX AND A TUMOR-TARGETING LIGAND IMPROVES TARGETED TRANSDUCTION

J de Vrij[1], IJC Dautzenberg[1], SK van den Hengel[1], MK Magnusson[2], TG Uil[1], SJ Cramer[1], J Vellinga[1], CS Verissimo[1], L Lindholm[2], D Koppers-Lalic[1] and RC Hoeben[1]

[1]Department of Molecular Cell Biology, Leiden University Medical Center, Leiden, The Netherlands and [2]Got-A-Gene AB, Kullavik, Sweden

Gene Therapy 2011; doi:10.1038/gt.2011.162

ABSTRACT

Human adenoviruses have a great potential as anticancer agents. One strategy to improve their tumor-cell specificity and anti-tumor efficacy is to include tumor-specific targeting ligands in the viral capsid. This can be achieved by fusion of polypeptide-targeting ligands with the minor capsid protein IX. Previous research suggested that protein IX-mediated targeting is limited by inefficient release of protein IX-fused ligands from their cognate receptors in the endosome. This thwarts endosomal escape of the virus particles. Here we describe that the targeted transduction of tumor cells is augmented by a cathepsin-cleavage site between the protein IX anchor and the HER2/neu-binding ZH Affibody molecule as ligand. The cathepsin-cleavage site did not interfere with virus production and incorporation of the Affibody molecules in the virus capsid. Virus particles harboring the cleavable protein IX-ligand fusion in their capsid transduced the HER2/neu-positive SKOV-3 ovarian carcinoma cells with increased efficiency in monolayer cultures, three-dimensional spheroid cultures and in SKOV-3 tumors grown on the chorioallantoic membrane of embryonated chicken eggs. These data show that inclusion of a cathepsin-cleavage sequence between protein IX and a high-affinity targeting ligand enhances targeted transduction. This modification further augments the applicability of protein IX as an anchor for coupling tumor-targeting ligands.

INTRODUCTION

Many clinical studies have demonstrated the feasibility and safety of cancer therapy with human adenovirus type 5 (HAdV-5)-derived vectors. However the efficacy of HAdV-5-based therapies still needs further enhancement. Several factors have been identified that limit the anti-tumor efficacy (reviewed in de Vrij *et al.*[1]). One of these is the inadequate penetration and spread of the therapeutic virus within the tumor. This might be attributable, at least in part, to the low or heterogeneous expression of the coxsackie and adenovirus receptor (CAR) on the tumor cells.[2,3] Much effort has been invested in devising strategies to improve the transduction efficiency of tumor cells *in situ*. Such strategies include the replacement of the HAdV-5 fibers with those of non-CAR binding HAdV serotypes, the inclusion of an integrin-binding arginine-glycine-aspartic acid (RGD) motif in the fiber to bypass the CAR dependency, and fusing capsid proteins with tumor-cell-binding polypeptides (reviewed in Bachtarzi *et al.*[4]). In the latter approach, adenovirus capsid proteins, such as fiber, penton-base, hexon and protein IX, have been explored as sites for inclusion of targeting polypeptides.

It has previously been demonstrated that fusion of peptides at the carboxy terminus of protein IX allows incorporation of peptides near the surface of the adenovirus capsid.[5,6] Incorporation of an α-helical spacer between the targeting peptide and the protein IX anchor increases the accessibility of the protein ligands on the virus surface.[6] The capsid-exposed domains of protein IX can be modified without negatively interfering with virus stability and infectivity, which is in contrast to fiber modifications.[7] So far, it has been demonstrated that large and complex proteins, such as single-chain antibodies, single-chain T-cell receptors, fluorescent proteins and herpes simplex virus thymidine kinase, can be fused with protein IX without losing their function.[8-10]

We have shown that enhanced transduction of tumor cells was obtained through fusing protein IX with an RGD domain,[6] thereby targeting cellular integrins, or through fusing protein IX with a single-chain T-cell receptor directed against MAGE-A1 cancer-testis antigens presented by HLA-A1 molecules.[9] However, with other ligands targeting efficiency was rather low, which led to the hypothesis that a protein IX-linked ligand requires dissociation from its cellular receptor after cellular uptake, to enable efficient targeted transduction.[11] In a normal infection the HAdV-5 particles are taken up in clathrin-coated endosomes after binding of the fiber-knob domains to the CAR receptor, and secondary binding of the penton-base RGD motifs to cellular integrins.[12-14] Thereafter, the CAR-bound fiber proteins are released from the virus capsid, thereby disconnecting the virus from the endosomal membrane.[15,16] This allows its release into the cytoplasm. During endosomal escape protein IX remains attached to the capsid without being subject of proteolytic degradation.[16] As a result, high-affinity binding between the protein IX-fused ligand and the receptor may cause inefficient endosomal release of the virus in the endosome.

Here we describe the development and evaluation of a mechanism for dissociation of the protein IX-fused ligand from the virus capsid. To facilitate the release of the vector particles from the cellular receptor, we introduced a cathepsin-cleavage site (ccs) between the protein IX anchor and the targeting ligand. Endosomes contain

high levels of cathepsin proteases, which become active upon acidification of the endosome (reviewed in Kirschke *et al.*[17]). The HER2/neu-binding ZH Affibody molecule was chosen as targeting ligand.[18] HER2/neu is overexpressed in many cancers, including cancers from the breast and prostate, and is therefore a potential target for cancer gene therapies.[19] The ZH Affibody molecule has been successfully employed for targeting of HAdV-5 to HER2/neu upon introduction in the fiber.[20]

Our assays revealed that introducing a ccs between protein IX and a ZH Affibody molecule does not interfere with virus production and incorporation of the ZH Affibody molecules into the virus capsid. The ccs-containing virus demonstrated significantly enhanced transduction of SKOV-3 ovarian carcinoma cells in cell culture models as well as in a chorioallantoic membrane (CAM) tumor model as compared to the non-ccs-containing control virus.

RESULTS

In vitro cleavage analyses on protein IX-ccs-ligand proteins

We first set out to explore the possibility of functionally incorporating a cathepsin-cleavable amino-acid sequence in a protein IX-ligand polypeptide fusion protein. To this end, the fusion proteins pIX.13R4.myc.his, pIX.ccsB.13R4.myc.his and pIX.ccsL.13R4.myc.his were purified and tested for their cathepsin sensitivity. The 13R4.myc.his polypeptide sequence (with 13R4 being a single-chain antibody fragment directed against β-galactosidase) has previously been successfully fused with protein IX.[8] A schematic overview of the fusion proteins is depicted in **Fig. 1a**.

Lentivirus vectors were used to generate 911 cell lines stably expressing the protein IX fusion proteins. The histidine (his) tag fused to 13R4 enabled the subsequent isolation of the fusion proteins via binding to nickel beads. Thereafter, the proteins were incubated with either cathepsin B or cathepsin L, and the cleavage products were analyzed by sodium dodecyl sulfate-polyacrylamide gel electrophoresis and immunoblotting (**Fig. 1b**). This revealed cleavage of the cathepsin L-cleavage site (ccsL)-containing fusion protein, as indicated by the appearance of the 25 kDa-sized fragment. The cathepsin B-cleavage site (ccsB)-containing protein was not cleaved. Of note, minor adjustments to the protocol (for example, cleavage of pIX.ccsL.13R4.myc.his after elution from the beads) resulted in pIX.ccsL.13R4.myc.his degradation without the appearance of a cleavage product (data not shown). Probably, the cathepsin L preparation (derived from human liver) contains contaminating levels of other proteases, which may degrade the cleavage protein. Cleavage of pIX.ccsL.13R4.myc.his could be blocked by co-incubation with the cathepsin-specific inhibitor Z-FY(t-Bu)-DMK (**Fig. 1b**).

The pIX.13R4.myc.his and pIX.ccsL.13R4.myc.his fusion proteins were incorporated in the capsid of HAdV-5 (**Fig. 1c**). Incorporation efficiency was similar for both fusion proteins, and the presence of the ccsL site did not result in detectable levels of protein cleavage. Importantly, after incorporation of the pIX.ccsL.13R4.myc.his into the HAdV-5 capsid, the fusion protein was still sensitive to cathepsin L (**Fig. 1d**), indicating that the ccsL was functional and accessible in the adenovirus capsid.

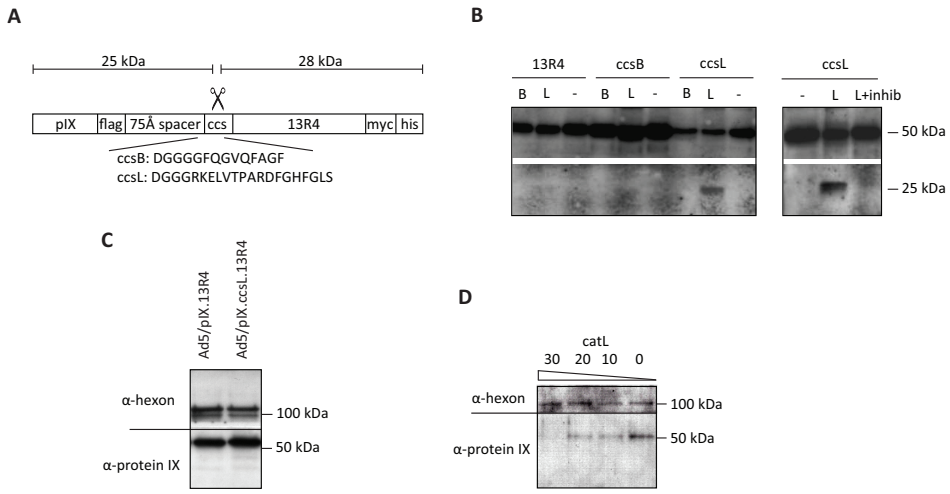

Figure 1. (**a**) Schematic representation of the pIX.13R4 fusion proteins. All polypeptide components are indicated (protein IX, flag tag, 75-Ångstrom spacer, ccs, 13R4 (single-chain antibody fragment directed against β-galactosidase), myc tag, his tag). (**b**) Western analyses after cathepsin cleavage of pIX.13R4 fusion proteins bound to nickel beads. The left panel indicates pIX.13R4 (13R4), pIX.ccsB.13R4 (ccsB) and pIX.ccsL.13R4 (ccsL) protein levels after cathepsin B (catB), cathepsin L (catL) or mock incubation. The right panel indicates pIX.ccsL.13R4 protein levels after cathepsin L cleavage in the presence or absence of the cathepsin inhibitor Z-FY(t-Bu)-DMK. Analyses were performed using anti-protein IX antibody. (**c**) Western analysis of pIX.13R4 and pIX.ccsL.13R4 protein levels after incorporation in the capsid of the protein IX-deleted HAdV mutant dl313 (5 x 10^9 pp per lane). Detection was carried out with anti-protein IX and anti-hexon antibodies. (**d**) Western analysis of pIX.ccsL.13R4 incorporated in the dl313 virus after incubation with different concentrations of cathepsin L (0, 10, 20 and 30 ng μl^{-1}) (5 x 10^9 pp per lane). Detection was carried out with anti-protein IX and anti-hexon antibodies.

Binding of Ad5/pIX.ccsL.ZH to the extracellular domain of HER2/neu

We and others have demonstrated that the HER2/neu-binding ZH Affibody molecules can be used for adenovirus targeting by incorporating these ligands in the HI loop of the adenovirus fiber.[20] Fusion of these Affibody domains with protein IX was far less efficient in retargeting adenovirus infection to HER2/neu-positive cells (our unpublished data). To study whether protein IX-Affibody-mediated targeting could be improved, we generated adenoviruses with protein IX-ccsL-ZH fusion proteins incorporated in their capsid, with the ccsL site located in between the 75-Ångstrom spacer and the tandem sequence of ZH Affibody molecules. By using standard cloning, recombination, and virus-rescuing procedures, we produced replication-competent HAdV-5 viruses with the sequences for pIX, pIX.ZH, or pIX.ccsL.ZH incorporated in the genome. In the viral genomes, major part of the E3 region was replaced by an enhanced GFP expression cassette.[21] The incorporation of the modified protein IX genes did not affect the titers (in physical particle (pp) ml^{-1} as well as plaque forming units (PFU) ml^{-1}) of the purified virus preparations (data not shown).

To investigate the functionality of the capsid-incorporated ZH Affibody molecules, a slot-blot-based HER2-ECD binding assay was performed (Fig. 2). Membrane-

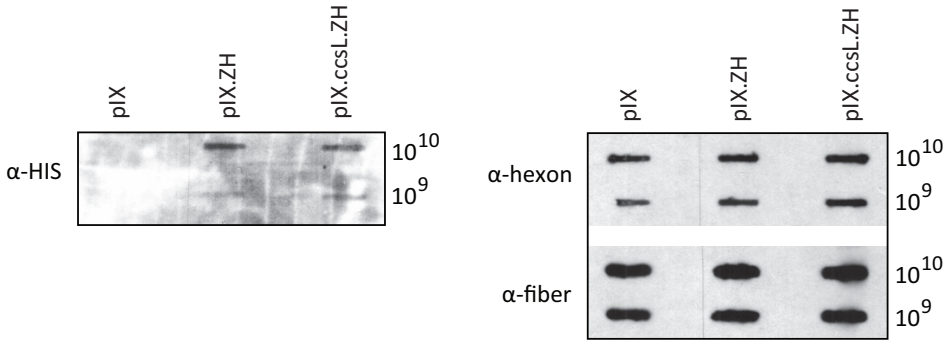

Figure 2. Slot-blot analyses of HER2-ECD binding to intact virus particles. HER2-ECD binding was assayed by subsequent incubation with his-tagged HER2-ECD and anti-HIS antibody. For loading-control purpose, incubation with anti-fiber-knob and anti-hexon antibody was performed. Two virus concentrations (10^{10} and 10^{9} pp) were applied to the membrane.

immobilized virus particles were incubated with soluble HER2-ECD, after which virus-bound HER2-ECD was detected by virtue of the his tag, which was fused with the HER2-ECD polypeptide. This experiment demonstrated binding of the HER2-ECD to Ad5/pIX.ZH and Ad5/pIX.ccsL.ZH particles. As expected, all viruses bound equivalent amounts of an antibody recognizing the fiber-knob domain. Also, the amounts of hexon antigen detected were similar, confirming equivalent particle loading in all samples. From these data, we conclude that both viruses with protein IX-Affibody fusions are functionally capable of binding HER2/neu.

Improved transduction of SKOV-3 cell culture by Ad5/pIX.ccsL.ZH

Subsequently, we studied the capacity of the viruses to transduce cultured cells that lack CAR but overexpress HER2/neu. Analyses were performed on the cell lines SKOV-3 (HER2/neu-positive and CAR-negative) and 911 (HER2/neu-negative and CAR-positive). Infection of SKOV-3 cells in an agar-overlaid monolayer culture showed the appearance of larger plaques for Ad5/pIX.ccsL.ZH (mean 2.4 arbitrary surface units (ASU), range 0.5-5.5), as compared to Ad5/pIX (mean 1.4 ASU, range 0.5-2.5) and Ad5/pIX.ZH (mean 0.9 ASU, range 0.5-2.5) (representative plaques are shown in **Fig. 3a**). No differences were observed between Ad5/pIX and Ad5/pIX.ZH, suggesting that the presence of the ccsL site had an effect on the efficiency of transduction of the HER2/neu-positive cells. In contrast, the plaques observed on monolayers of 911 cells had a similar size distribution for all three viruses (mean 1.3 ASU, range 0.5-4.5 for Ad5/pIX, mean 1.3 ASU, range 0.5-3.5 for Ad5/pIX.ZH, mean 1.4 ASU, range 0.5-3.5 for Ad5/pIX.ccsL.ZH). These data suggest that inclusion of the pIX.ccsL.ZH in the capsid enhanced the virus spread in monolayers of CAR-negative, HER2/neu-positive cells.

To test whether the infection is also enhanced in three-dimensional tumor cell cultures, the viruses were applied on SKOV-3 and 911 spheroids (**Fig. 3b**). As in the SKOV-3 monolayer cultures, Ad5/pIX.ccsL.ZH displayed the highest transduction efficiency on SKOV-3 spheroids, with the GFP expression levels being significantly higher than the levels obtained after Ad5/pIX and Ad5/pIX.ZH infection. As expected,

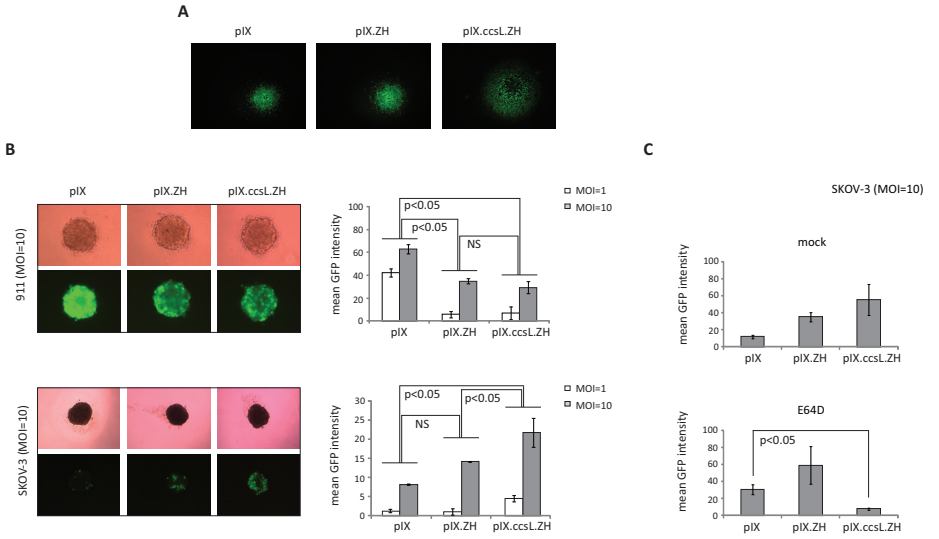

Figure 3. (**a**) Plaque assay to compare Ad5/pIX, Ad5/pIX.ZH and Ad5/pIX.ccsL.ZH infection of monolayer cell cultures. The microscopy pictures show representative GFP-positive SKOV-3 plaques. (**b**) Transduction of 911 and SKOV-3 spheroids with Ad5/pIX, Ad5/pIX.ZH and Ad5/pIX.ccsL.ZH. Infection was performed at multiplicities of infection (MOI) of 1 and 10 PFU per cell. The graphs show the mean GFP intensities at 5 days post-transduction. Error bars represent s.d. (n = 3). Differences in GFP intensity are considered significant at P<0.05 for both MOIs. Representative pictures (at 5 days post-transduction) are shown on the left. (**c**) Transduction of SKOV-3 spheroids with Ad5/pIX, Ad5/pIX.ZH and Ad5/pIX.ccsL.ZH in the presence or absence of the cysteine protease inhibitor E64-D. The graphs show the mean GFP intensities at 5 days post-transduction. Error bars represent s.d. (n = 3).

no enhanced transgene delivery was observed for the Ad5/pIX.ccsL.ZH virus on the non-target 911 spheroids. Strikingly, the transduction efficiencies for both ZH-containing viruses appeared reduced on the 911 spheroids, as compared with the transduction efficiency for Ad5/pIX. This reduction is in contrast to the results obtained on the 911 monolayers, which showed identical plaque sizes for all three viruses. The cause for this discrepancy between the monolayer and the spheroid model remains to be elucidated. It is conceivable that the growth of the cells in such different conditions affects the cell surface expression or accessibility of the viral receptors CAR and integrins. Irrespective of the mechanism, the reduced transduction of Ad5/pIX.ZH and Ad5/pIX.ccsL.ZH on the non-target 911 spheroids may result from the presence of large targeting ligands fused with protein IX. This warrants further investigation.

The enhanced GFP expression upon Ad5/pIX.ccsL.ZH infection of SKOV-3 spheroids could be inhibited by incubation with the cysteine-protease-specific inhibitor E64-D (**Fig. 3c**). Although the presence of the inhibitor resulted in a modest increase in transduction for Ad5/pIX and Ad5/pIX.ZH, the transduction efficiency for Ad5/pIX.ccsL.ZH was strongly decreased. Of interest, the addition of the cathepsin inhibitor resulted in a general effect on SKOV-3 spheroid morphology, with obvious changes in the cell density on the spheroid surface (results not shown). This effect

probably caused the modest increase in transduction for the Ad5/pIX and Ad5/pIX.ZH viruses.

Analysis of transduction of SKOV-3 tumors on a CAM

To gain insight into the performance of the viruses *in vivo*, the viruses were tested for their transduction efficiencies in human tumors grown on the CAM of embryonated chicken eggs. The engraftment of SKOV-3 cells at embryo development day 7 (EDD7) resulted in the rapid formation of tumors with a size of 4-6 mm at EDD14 (= day of virus injection), with obvious appearance of blood vessel sprouting (**Fig. 4a**). Western analysis was carried out at EDD14 to analyze the expression of cathepsin L in the CAM tumor lysate (**Fig. 4b**). Pro-cathepsin L (42 kDa) as well as the active form of cathepsin L (25 kDa) were detected. At EDD20 (=6 days post virus injection), the tumors were harvested and GFP signals were quantified (**Fig. 4c**). The insertion of the ccsL site significantly enhanced transduction, with the GFP expression level for Ad5/pIX.ccsL.ZH being approximately twice the levels as seen with Ad5/pIX and Ad5/pIX.ZH.

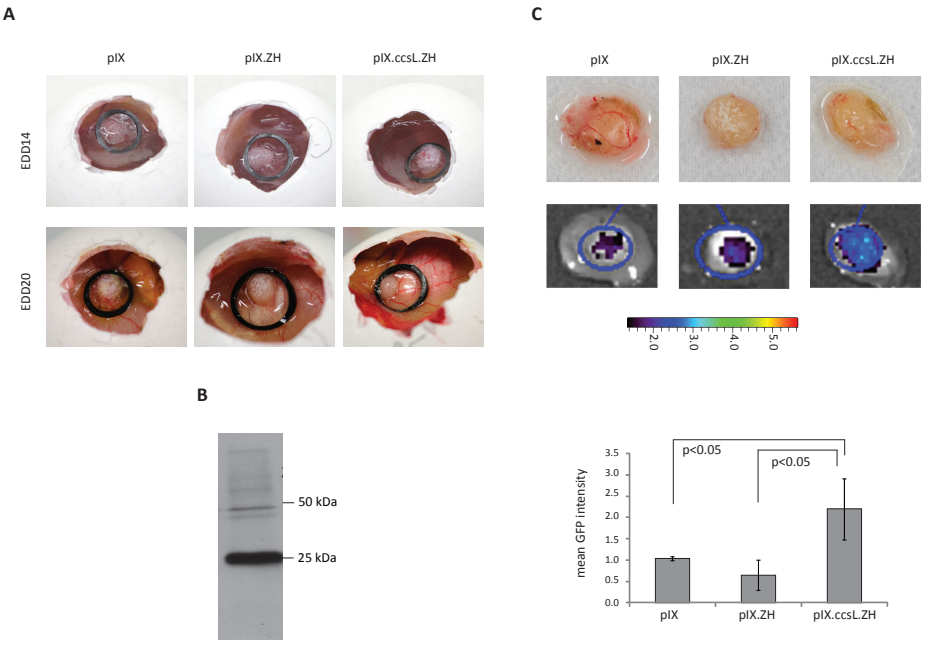

Figure 4. Virus transduction of SKOV-3 cells grown on the CAM. (**a**) Representative pictures of CAM tumors at EDD 14 (before virus injection) and EDD 20 (before tumor isolation). (**b**) Western analysis of cathepsin L protein levels in lysates of SKOV-3 cells grown as CAM tumor. Detection was carried out with anti-cathepsin L antibody directed against pro-cathepsin L (42 kDa) as well as the active form of cathepsin L (25 kDa). (**c**) Biofluorescent imaging with the IVIS system of GFP expression in SKOV-3 tumors retrieved from the CAM (EDD 20). The graph shows the mean GFP intensities. Error bars represent s.d. (*n* = 5). Representative IVIS pictures are included.

DISCUSSION

We studied the usability of cathepsin-cleavage sites in mediating the dissociation of HAdV-5 protein IX from fused tumor-targeting ligands. Inclusion of a ccsL in between protein IX and a HER2/neu-targeted ZH Affibody molecule enhanced the transduction of HER2/neu-positive SKOV-3 tumor cells. The enhanced delivery of an *enhanced* GFP reporter gene was observed in monolayer culture, three-dimensional spheroid culture, as well as in SKOV-3 tumors grown on the CAM of embryonated chicken eggs. These results provide a strategy to enhance the applicability of protein IX as an anchor for coupling high-affinity tumor-targeting ligands.

Varying efficiencies have been reported for protein IX-mediated retargeting approaches, with the targeted transduction efficiency depending on the type of ligand used.[9,11,22] It was first suggested by Barry *et al*.[11] that high-affinity binding between a protein IX-coupled targeting ligand and its receptor may prevent release of the virus particle from the targeted receptor, resulting in inefficient escape of the virus particle from the endosome to the cytoplasm. Such endosomal sequestration is in contrast to fiber-mediated targeting, as the fiber is released from the virus particle upon cellular uptake.[15,16] To gain more insight into the phenomenon of endosomal entrapment of protein IX targeted HAdV-5 vectors, Corjon *et al*.[22] fused protein IX with the RAP (receptor-associated protein) ligand, which is evolutionary designed for dissociation from its target receptor (LRP; LDL-receptor-related protein) at low pH. As intended, this strategy resulted in proper routing of the virus particles in the LDL-expressing target cells (from endosome to the nuclear periphery), and retargeting efficiency appeared to be equal to fiber-RAP-mediated retargeting of HAdV-5.

To prevent the endosomal entrapment of protein IX-targeted HAdV-5, we set out to test whether insertion of a ccs can be used to circumvent this problem, by facilitating endosomal release of the vector. Such mechanism would mimic the strategies adopted by other viruses. Reovirus is disassembled by cathepsins B and L in the endosome. This is a crucial step in its infective pathway.[23] The Ebola virus is dependent on cleavage of glycoprotein GP1 by cathepsins B and L to trigger membrane fusion and cell entry.[24] In addition, activation of the Nipah virus fusion protein (responsible for virus entry into the host cell) is mediated by endosomal proteases, presumably cathepsins.[25] Ccs incorporation has already been introduced in radioimmunotherapy, which has revealed a decrease in hepatic toxicity when a cathepsin cleavable peptide is attached to the therapeutic-chelated radiometal.[26]

We first performed an *in vitro* cleavage assay to compare a ccsB and a ccsL site for their cleavage sensitivity if incorporated in between protein IX and a model ligand, that is, the hyper-stable single-chain antibody fragment 13R4.[8] Cathepsins B and L, which belong to the papain-like family of cysteine proteases, are ubiquitous in the lysosomes of animals.[27] The enzymes are endopeptidases, although cathepsin B was found also to be a dipeptidyl carboxypeptidase.[28] Among the lysosomal cysteine proteases, cathepsin L was found to be the most active in degradation of protein substrates[27,29,30] and cathepsin B the most abundant.[27] The enzymes are optimally active at slightly acidic pH, that is, pH 6.0 for cathepsin B and pH 5.5 for cathepsin L (reviewed in Kirschke *et al*.[17]). This allows full activity within the lysosomal and endosomal compartments. Interestingly, and probably of relevance to our strategy

of using a ccs in HAdV-5 tumor targeting, cathepsins are frequently up regulated in human cancers, and have been implicated in distinct tumorigenic processes such as angiogenesis, proliferation, apoptosis and invasion (reviewed in Gocheva and Joyce[31]).

Our assays demonstrated that the pIX.ccsL.ligand fusion molecule was efficiently inserted in the HAdV-5 capsid. The ccsL site retained its sensitivity for cleavage with cathepsin L. Subsequently, the ccsL site was introduced in the genome of the replication-competent virus Ad5/pIX.ZH, between the protein IX and a tandem pair of ZH Affibody ligands. Binding of the soluble HER2-ECD to the particles was confirmed, demonstrating that the ZH Affibody molecules are located at an assessable location within the virus capsid. Furthermore, Ad5/pIX.ZH and Ad5/pIX.ccsL.ZH bound the HER2-ECD with similar efficiency, demonstrating that during virus production the virus particles were not exposed to active cathepsin L to an extend that leads to proteolytic removal of the targeting ligands.

By quantifying GFP expression levels, we compared the transduction efficiencies of the viruses Ad5/pIX, Ad5/pIX.ZH and Ad5/pIX.ccsL.ZH in different SKOV-3 models. In all models the mere presence of the ZH Affibody molecule was insufficient for significantly improving transduction efficiency. Insertion of the ccsL site, however, resulted in a significantly enhanced transduction in all SKOV-3 models tested. The targeted transduction efficacy was moderately but significantly enhanced in the spheroid as well as in the CAM tumor model.

Of interest, the transduction efficiencies of the ZH-containing viruses were significantly reduced, as compared to the Ad5/pIX virus, on the non-target (CAR-positive/HER2-negative) 911 cells in the three-dimensional spheroid model. The cause of this reduction, which is in contrast to the equal plaque sizes for all viruses in 911 monolayers, is unknown. One explanation might be that the wild-type HAdV-5 receptors (that is, CAR and/or integrins) are relatively poorly accessible on the cell surface in a 911-cell spheroid. As a consequence, extensive HAdV-5 capsid modification, such as the protein IX-ZH incorporation, might lead to changes in virion composition that restrict virus mobility to their receptors. Fusion of other ligands with protein IX can result in reduced transduction of 911 spheroids as well (our unpublished data), demonstrating that the effect is not specific for ZH Affibody molecules. It will be of interest to further analyze protein IX-ligand-targeted HAdV-5 vectors for their infection efficacy on non-target cells, for example, in human tumor xenografts in mice.

In this particular proof-of-principle study, the incorporation of a cathepsin L-cleavage site resulted in substantial improved transduction of SKOV-3 tumor cells. It remains to be established which ccs is optimally suited for a particular ligand and target combination. Tumor cell lines as well as primary tumors have been shown to strongly vary in their expression profile and expression level of the different types of cathepsins (BioGPS Gene Portal;[32] NCI60 cell lines (U133A) data set[33] and Human Primary Tumors (U95) data set[34]). Depending on the tumor type to target, the optimal ccs for incorporation in a pIX.ccs.ligand-containing HAdV-5 may vary, thereby necessitating preclinical ccs evaluations in oncolytic virus protocol development.

The causal mechanistic for the improved performance of the ccsL containing virus remains to be established. Although enhanced endosomal escape of the targeted viruses seems a plausible hypothesis, further studies are necessary to provide a definite answer. Despite these uncertainties on the mechanism, our results demonstrate the

feasibility of using a ccs for improving transgene delivery with protein IX-ligand-targeted HAdV-5 vectors. Enhanced transduction was observed in a spheroid and CAM tumor model, which are highly suitable models for analysis of transgene delivery in a three-dimensional context. Nevertheless, future experiments, implementing *bona fide* tumor models that allow long-term follow-up, will be necessary to reveal whether incorporation of a ccs leads to enhanced anti-tumor efficacy of protein IX-ligand-targeted viruses.

Our cathepsin-cleavage strategy enhances the potential for protein IX-mediated targeting of HAdV-based oncolytic viruses for cancer therapy. Also, the introduction of a ccs might be efficacy-improving for other (non-protein IX-based) HAdV-5 targeting approaches. It would be highly interesting to analyze the effect of introducing a ccs in fiber-ZH viruses,[20] and to perform a side-by-side comparison between pIX.ccs.ZH viruses and fiber-ccs-ZH viruses.

Future research will reveal whether protein IX-based targeting, in combination with other targeting (for example, fiber-ligand-based) and de-targeting approaches (for example, ablating CAR-binding by fiber knob modification or blood-coagulation factor X-binding by hexon modification[35]), can lead to improved oncolytic HAdV vectors. Such rational design strategies, as well as parallel strategies involving random mutagenesis and bioselection methodologies,[36-39] will facilitate the derivation of new targeted adenoviruses with improved tumor-cell specificity and anti-tumor efficacy.

MATERIALS AND METHODS

Cell lines

The human cell lines SKOV-3 (ovarian adenocarcinoma), A549 (carcinomic alveolar epithelium) and 911 (HAdV-5 E1-transformed embryonic retinoblasts)[40] were maintained at 37°C in a humidified atmosphere of 5% CO_2 in Dulbecco's Modified Eagle's Medium (Gibco-BRL, Breda, The Netherlands) supplemented with 8% fetal bovine serum (Gibco-BRL, Breda, The Netherlands) and penicillin-streptomycin.

Viruses

Overlap extension-polymerase chain reaction (PCR) (with oligonucleotides 1-4; **Table 1**) was used to fuse a tandem of ZH Affibody sequences derived from the plasmid FibR7-ZHZH,[20] with the sequence pIX.flag.75 derived from the plasmid pAd5pIX.flag.75.MYC.[6] Next, the resulting fusion fragment pIX.flag.75.(ZH)2 was flanked at both ends with a short sequence containing a restriction site (*Mlu*I upstream of the pIX.flag.75.(ZH)2 start codon and *Bst*Z17I downstream of the pIX.flag.75.(ZH)2 stop codon) by PCR. The pIX.flag.75.(ZH)2 sequence was ligated to the *Mlu*I- and *Bst*Z17I-digested plasmid pLV-CMV-IRES-NPTII,[41] resulting in the plasmid pLV-CMV-pIX.flag.75.(ZH)2-IRES-NPTII (pLV-pIX.ZH). Subsequently, a unique *Pac*I restriction site was introduced between the 75-Ångstrom spacer and the (ZH)2 sequence (with oligonucleotides 5 and 6; **Table 1**) by site-directed mutagenesis PCR, resulting in the plasmid pLV-CMV-pIX.flag.75.*Pac*I.(ZH)2-IRES-NPTII. The *Pac*I site enabled introduction of a cathepsin L-cleavage site by ligation of the annealed oligonucleotides 7 and 8 (**Table 1**), resulting in pLV-CMV-pIX.flag.75.ccsL.(ZH)2-IRES-NPTII (pLV-pIX.ccsL.ZH). The coding sequences of pIX.flag.75.

Table 1. Oligonucleotide list.

	Oligonucleotide	Sequence (5′ to 3′)
1	FWD Tthiii-pIX	TACGAGACCGTGTCTGGAACG
2	REV pIX75Å	GGCGCCGTGTAAGGTTGGGTTGTGGCGTTTGAAGGCGGCTTC
3	FWD pIX75Å-ZH	AACCCAACCTTACACGGCGCCGTAGACAACAAATTCAACAAA
4	REV DraI-ZH	GTTTTAAACTTTCGGCGCCTGAGCATCATT
5	FWD PacI-ZH	CAAACGCCACAACCCAACCTTAATTAAGGCCGTAGACAACAAATTC
6	REV PacI-ZH	GAATTTGTTGTCTACGGCCTTAATTAAGGTTGGGTTGTGGCGTTTG
7	FWD CatL-ZH	CGACGGCGGAGGGAGGAAGGAATTGGTGACGCCAGCACGAGA-CTTCGGTCATTTTGGATTATCCGGAGGCGGGAT
8	REV CatL-ZH	CCCGCCTCCGGATAATCCAAAATGACCGAAGTCTCGTGCTGGCGT-CACCAATTCCTTCCTCCCTCCGCCGTCGAT
9	FWD ScaI-pIX	CGCGGAAGTACTATGAGCACCAACTCGTTTGATGG
10	REV SpeI-ZH	CGCACTAGTCTAAACTTTCGGCGCCTGAGCAT
11	REV SpeI-pIX	CGCACTAGTTTAAACCGCATTGGGAGGGGAGG
12	FWD PacI-13R4	CAACCCAACCTTAAGCGCCGTCGACGGCTTAATTAACGGCG-GAGGGAGCATGG
13	REV PacI-13R4	CCATGCTCCCTCCGCCGTTAATTAAGCCGTCGACGGCGCTTA-AGGTTGGGT
14	FWD CatB-13R4	TCGACGGCGGAGGGGGCTTCCAGGGCGTGCAGTTCGCCG-GCTTCAT
15	REV CatB-13R4	GAAGCCGGCGAACTGCACGCCCTGGAAGCCCCCTCCGCCG
16	FWD CatL-13R4	TCGACGGCGGAGGGAGGAAGGAATTGGTGACGCCAGCACGAGA-CTTCGGTCATTTTGGATTATCCAT
17	REV CatL-13R4	GGATAATCCAAAATGACCGAAGTCTCGTGCTGGCGTCAC-CAATTCCTTCCTCCCTCCGCCG

Abbreviations: CatB, cathepsin B; CatL, cathepsin L; FWD, forward; pIX, protein IX; REV, reverse.

(ZH)2 and pIX.flag.75.ccsL.(ZH)2 were isolated from, respectively, pLV-pIX.ZH and pLV-pIX.ccsL.ZH by PCR (oligonucleotides 9 and 10; **Table 1**). The sequence for HAdV-5 protein IX was isolated from the plasmid pAd5pIX[6] by PCR with oligonucleotides 9 and 11 (**Table 1**). The *Sca*I-*Spe*I-flanked PCR products were cloned in pShuttle+E1+pIX$^{ScaI/SpeI}$.[42] The *Sca*I restriction site was restored by exchanging the E1B/protein IX sequence containing *Mfe*I/*Hind*III region with the corresponding fragment from pTG3602. The resulting plasmids pSh+pIX, pSh+pIX.ZH and pSh+pIX.ccsL.ZH were recombined with the HAdV-5-based backbone plasmid pBB[42] (containing the *eGFP* gene in the E3 region, based on the previously described pShuttle-ΔE3-ADP-EGFP-F2[21]), followed by virus rescue in A549 cells. Recombination and virus rescue were as described elsewhere.[42] The viruses (named Ad5/pIX, Ad5/pIX.ZH and Ad5/pIX.ccsL.ZH) were purified by a standard double cesium chloride gradient protocol, dialyzed against sucrose buffer (5% sucrose, 140 mM NaCl, 5 mM Na_2-HPO_4.$2H_2O$, 1.5 mM KH_2PO_4) and stored at −80 °C. The virus titer was determined by the PicoGreen-DNA binding assay[43] (for

pp ml^{-1} measurement), and a plaque assay on 911 cells (for PFU ml^{-1} measurement), as described in Fallaux *et al.*[40] To compare the virus spread in monolayers of 911 and SKOV-3 cells, standard plaque assays were performed, followed by photographing GFP-positive plaques and measuring plaque size with ImageJ software (National Institutes of Health, Bethesda, MD, USA). The plaque surface area of Ad5/pIX.ZH and Ad5/pIX.ccsL.ZH was normalized to the plaque surface area of Ad5/pIX.

Western analyses

Cell lysates were made in radioimmunoprecipitation assay lysis buffer (50 mM Tris-Cl, pH 7.5, 150 mM NaCl, 0.1% sodium dodecyl sulfate, 0.5% DOC, and 1% NP40) supplemented with protease inhibitors. Protein concentrations were determined with a BCA protein assay (Pierce, Etten-Leur, The Netherlands). Cell lysate samples for western analysis were prepared by boiling of 20 µg of total protein in reducing sample buffer (final composition: 33 mM Tris-Cl, pH 6.7, 9% glycerol, 2% sodium dodecyl sulfate and 2.2% β-mercaptoethanol, and 2.2% from a 1:20 dilution of a saturated bromophenol blue solution) for 5 min at 100°C. Virus samples for western analysis were prepared by adding purified viruses directly to the reducing sample buffer, followed by boiling. All samples were subjected to standard sodium dodecyl sulfate-polyacrylamide gel electrophoresis, with 15% polyacrylamide running gels, and subsequent protein transfer to polyvinylidene difluoride (PVDF) membranes (Immobilon-P transfer membrane; Millipore, Amsterdam, The Netherlands) by electroblotting. After immunological probing of the blots, horse radish peroxidase (HRP)-conjugated antibodies were detected by enhanced chemiluminescence. Primary antibodies used were goat polyclonal anti-hexon (1:2000, ab19998; Abcam, Cambridge, UK), rabbit polyclonal anti-protein IX (1:2000)[44], and mouse monoclonal anti-cathepsin L (1:500, [33/2] ab6314; Abcam). Secondary antibodies used were HRP-conjugated goat-anti-rabbit and mouse-anti-goat (Santa Cruz Biotechnology, Santa Cruz, CA, USA).

In vitro cathepsin cleavage assay

To test various protein sequences for their usage as ccs in the context of a protein IX-ligand incorporation, we introduced the sequences in our previously described pIX.13R4.myc.his fusion protein[8] (**Fig. 1a**). To this end, PCR was carried out (with oligonucleotides 12 and 13; **Table 1**) to introduce a *Pac*I site in the plasmid pLV-CMV-pIX.flag.75.13R4.myc.his-IRES-NPTII (pLV-pIX.13R4.myc.his).[8] Subsequently, oligonucleotides 14 and 15 (**Table 1**) were used for insertion of a ccsB[45] and oligonucleotides 16 and 17 (**Table 1**) for insertion of a ccsL,[23] resulting in the plasmids pLV-pIX.ccsB.13R4.myc.his and pLV-pIX.ccsL.13R4.myc.his. From the pLV plasmids recombinant lentiviruses were produced, which were subsequently used for transduction of 911 cells to establish the expression of proteins pIX.13R4.myc.his, pIX.ccsB.13R4.myc.his, and pIX.ccsL.13R4.myc.his. Lentivirus production and the transduction of 911 cells were performed as described previously.[41]

After lysing the 911 cells with radioimmunoprecipitation assay lysis buffer, the protein IX fusion proteins were bound to nickel beads (IBA, Qiagen, Valencia, CA, USA), enabled by the presence of the his tag fused to the 13R4 ligand. Cell lysates (40 µg) were incubated overnight at 4°C with 20 µl NI-NTA beads and wash buffer (50 mM

$Na_2H_2PO_4$, 300 mM NaCl, 20 mM immidazole, pH 8.0) was added to a final volume of 1 ml. After one washing step with 1 ml wash buffer, the beads were re-suspended in 50 µl cathepsin digestion buffer (50 mM sodium acetate buffer, 2 mM EDTA, 2 mM dithiothreitol, pH 5.0).

Purified virus particles with the protein IX-ligand proteins incorporated in the capsid were prepared by using our previously described strategy involving the infection of protein IX-producing cell lines with a protein IX gene lacking HAdV-5.[41] Briefly, the virus was prepared by infecting the protein IX-ligand-expressing 911 cell lines with the HAdV-5 dl313 mutant, followed by harvesting, purification, and storage of the offspring virus. The sucrose-based storage buffer of the virus preparation was exchanged for cathepsin cleavage buffer by filter centrifugation (Amicon Ultra-4 filter tubes; Millipore). Aliquots of 50 µl, containing 5 x 10^9 pp (as determined by the PicoGreen-DNA binding assay) were prepared for cathepsin cleavage analysis.

Cathepsin cleavage was tested by incubation with cathepsin L (human, liver; Merck KGaA, Darmstadt, Germany) (28,6 ng/µl) or cathepsin B (human, liver, Merck KGaA) (250 ng/µl) for 1 h at 37°C. The samples were subjected to western blotting for the analysis of protein cleavage. Cathepsin L cleavage was inhibited with 10 µM specific inhibitor Z-FY(t-Bu)-DMK (Merck KGaA).

Slot-blot-based assay for analysis of HER2-ECD binding to intact virus particles

Binding of purified virions to the HER2/neu ECD (HER2-ECD) was assessed by a slot-blot-based protocol as described by Uil *et al*.[46] In brief, the virions were diluted in PBS and blotted onto a polyvinylidene difluoride membrane (Millipore) using a slot-blot apparatus. Blocking was carried out with 2.5% bovine serum albumin, 2.5% protifar (Nutricia, Zoetermeer, The Netherlands) in PBS for 2 h. Functional presentation of HER2/neu on the virion surface was analyzed by overnight incubation with HER2-ECD (300 ng/ml) (Fox Chase Cancer Centre, Philadelphia, PA, USA). The presence of a his tag fused to HER2-ECD allowed the subsequent immunological staining with HRP-conjugated goat polyclonal anti-his tag antibody (ab1269; Abcam). In parallel, staining was performed with mouse anti-fiber-knob (1D6.14 (1:250))[47] and goat anti-hexon antibody (1:2000, ab19998; Abcam), followed by incubation with HRP-conjugated secondary antibodies.

Spheroid analysis

Semiconfluent 911 cells and SKOV-3 cells were trypsinized, counted, and re-suspended in medium containing 2.4 mg/ml methylcellulose (Sigma Aldrich Chemie, Zwijndrecht, The Netherlands) at the concentration of 10^4 cells/ml. Cell suspension (100 µl) was added into each well of a U-bottom 96-well-plate allowing the formation of one spheroid (consisting of 10^3 cells) per well. Viral infection was initiated at two days after plating by exchanging the medium with infectious medium (multiplicity of infection =1 or 10 PFU per cell). After 2 h, the infectious medium was replaced with normal medium. To test the dependency of transduction on cathepsin L activity, the cysteine protease inhibitor E64-D (Sigma Aldrich) was added to the infectious medium at a concentration of 5 µg/ml. Pictures were taken at 5 days after infection (Olympus Camedia Digital Camera C-3030, installed on an Olympus CK40 microscope) and transduction was quantified by measuring the mean GFP intensity using ImageJ software.

Chicken CAM assay

Human tumors were grown on the chicken CAM as described in detail by Durupt *et al*.[48] Briefly, fertilized chicken eggs (*Gallus domesticus*) were placed in a humidified incubator at 37°C without CO_2 to induce embryogenesis (EDD 0). On EDD 4, a small hole was made with a 19G needle in the air sack and a window was cut using a forceps under sterile conditions. The shell membrane was humidified with sterile PBS and carefully removed. This window was then sealed with a 3 cm Petri dish and eggs were placed back to the incubator. At day 7 (EDD 7), viability of the embryos and the vasculature of the CAM were visually inspected and the CAM was gently lacerated with a sterile cotton swab to create a blood spot to facilitate engraftment of tumor cells. Tumor cells were collected by trypsinization, washed with culture medium and pelleted by gentle centrifugation. After removing the medium, 10^7 SKOV-3 cells were resuspended in 50 µL matrigel (Growth-Factor Reduced Matrigel; Becton-Dickinson, Breda, The Netherlands) and inoculated on the CAM. Eggs were sealed, placed back into the incubator, and tumor growth was inspected on a daily basis. Purified virus (1 µl, 10^4 PFU) was injected at EDD 14 in the center of each tumor mass using a 30G syringe. At EDD 20, the eggs were placed on ice for at least 2 h to euthanize the chick embryos by hypothermia and tumors were isolated and collected in a Petri dish for immediate analyses of GFP expression with a Xenogen IVIS 100 biofluorescence imaging system (Xenogen, Alameda, CA, USA). For the analysis of cathepsin L expression, three tumors (not infected with virus) were transferred at EDD14 to a tube with 2 ml radioimmunoprecipitation assay lysis buffer, followed by sonication at 4°C. The cell debris was removed by centrifugation, and the supernatants were stored at -20°C for western analysis.

ACKNOWLEDGEMENTS

We thank Masato Yamamoto (Department of Surgery, University of Minnesota, MN, USA) for providing us with the plasmid pShuttle-ΔE3-ADP-EGFP-F2. In addition, Ivo Que (Department of Endocrinology, Leiden University Medical Center, Leiden, The Netherlands) is gratefully acknowledged for precious technical assistance in the biofluorescence experiments. This work was supported by the European Union through the 6th Framework Program GIANT (Contract No. 512087).

REFERENCES

1. de Vrij J, Willemsen RA, Lindholm L, Hoeben RC, Bangma CH, Barber C *et al*. Adenovirus-derived vectors for prostate cancer gene therapy. *Hum Gene Ther* 2010; **21:** 795-805.
2. Li D, Duan L, Freimuth P, O'Malley BW, Jr. Variability of adenovirus receptor density influences gene transfer efficiency and therapeutic response in head and neck cancer. *Clin Cancer Res* 1999; **5:** 4175-4181.
3. Hemmi S, Geertsen R, Mezzacasa A, Peter I, Dummer R. The presence of human coxsackievirus and adenovirus receptor is associated with efficient adenovirus-mediated transgene expression in human melanoma cell cultures. *Hum Gene Ther* 1998; **9:** 2363-2373.
4. Bachtarzi H, Stevenson M, Fisher K. Cancer gene therapy with targeted adenoviruses. *Expert Opin Drug Deliv* 2008; **5:** 1231-1240.
5. Dmitriev IP, Kashentseva EA, Curiel DT. Engineering of adenovirus vectors containing heterologous peptide sequences in the C terminus of capsid protein IX. *J Virol* 2002; **76:** 6893-6899.
6. Vellinga J, Rabelink MJ, Cramer SJ, van den Wollenberg DJ, Van der Meulen H, Leppard KN *et al*. Spacers increase the accessibility of peptide ligands linked to the carboxyl terminus of adenovirus minor capsid protein IX. *J Virol* 2004; **78:** 3470-3479.
7. Vellinga J, van den Wollenberg DJ, van der Heijdt S, Rabelink MJ, Hoeben RC. The coiled-coil domain of the adenovirus type 5 protein IX is dispensable for capsid incorporation and thermostability. *J Virol* 2005; **79:** 3206-3210.
8. Vellinga J, de Vrij J, Myhre S, Uil T, Martineau P, Lindholm L *et al*. Efficient incorporation of a functional hyper-stable single-chain antibody fragment protein-IX fusion in the adenovirus capsid. *Gene Ther* 2007; **14:** 664-670.
9. de Vrij J, Uil TG, van den Hengel SK, Cramer SJ, Koppers-Lalic D, Verweij MC *et al*. Adenovirus targeting to HLA-A1/MAGE-A1-positive tumor cells by fusing a single-chain T-cell receptor with minor capsid protein IX. *Gene Ther* 2008; **15:** 978-989.
10. Tang Y, Wu H, Ugai H, Matthews QL, Curiel DT. Derivation of a triple mosaic adenovirus for cancer gene therapy. *PLoS One* 2009; **4:** e8526.
11. Campos SK, Barry MA. Comparison of adenovirus fiber, protein IX, and hexon capsomeres as scaffolds for vector purification and cell targeting. *Virology* 2006; **349:** 453-462.
12. Bergelson JM, Cunningham JA, Droguett G, Kurt-Jones EA, Krithivas A, Hong JS *et al*. Isolation of a common receptor for Coxsackie B viruses and adenoviruses 2 and 5. *Science* 1997; **275:** 1320-1323.
13. Nemerow GR, Stewart PL. Role of alpha(v) integrins in adenovirus cell entry and gene delivery. *Microbiol Mol Biol Rev* 1999; **63:** 725-734.
14. Wickham TJ, Mathias P, Cheresh DA, Nemerow GR. Integrins alpha v beta 3 and alpha v beta 5 promote adenovirus internalization but not virus attachment. *Cell* 1993; **73:** 309-319.
15. Sussenbach JS. Early events in the infection process of adenovirus type 5 in HeLa cells. *Virology* 1967; **33:** 567-574.
16. Greber UF, Willetts M, Webster P, Helenius A. Stepwise dismantling of adenovirus 2 during entry into cells. *Cell* 1993; **75:** 477-486.
17. Kirschke H, Barrett AJ, Rawlings ND. Proteinases 1: lysosomal cysteine proteinases. *Protein Profile* 1995; **2:** 1581-1643.
18. Wikman M, Steffen AC, Gunneriusson E, Tolmachev V, Adams GP, Carlsson J *et al*. Selection and characterization of HER2/neu-binding affibody ligands. *Protein Eng Des Sel* 2004; **17:** 455-462.
19. Wang SC, Hung MC. HER2 overexpression and cancer targeting. *Semin Oncol* 2001; **28:** 115-124.
20. Magnusson MK, Henning P, Myhre S, Wikman M, Uil TG, Friedman M *et al*. Adenovirus 5 vector genetically re-targeted by an Affibody molecule with specificity for tumor antigen HER2/neu. *Cancer Gene Ther* 2007; **14:** 468-479.
21. Ono HA, Le LP, Davydova JG, Gavrikova T, Yamamoto M. Noninvasive visualization of adenovirus replication with a fluorescent reporter in the E3

region. *Cancer Res* 2005; **65:** 10154-10158.

22. Corjon S, Wortmann A, Engler T, van Rooijen N, Kochanek S, Kreppel F. Targeting of adenovirus vectors to the LRP receptor family with the high-affinity ligand RAP via combined genetic and chemical modification of the pIX capsomere. *Mol Ther* 2008; **16:** 1813-1824.
23. Ebert DH, Deussing J, Peters C, Dermody TS. Cathepsin L and cathepsin B mediate reovirus disassembly in murine fibroblast cells. *J Biol Chem* 2002; **277:** 24609-24617.
24. Schornberg K, Matsuyama S, Kabsch K, Delos S, Bouton A, White J. Role of endosomal cathepsins in entry mediated by the Ebola virus glycoprotein. *J Virol* 2006; **80:** 4174-4178.
25. Diederich S, Moll M, Klenk HD, Maisner A. The nipah virus fusion protein is cleaved within the endosomal compartment. *J Biol Chem* 2005; **280:** 29899-29903.
26. DeNardo GL, DeNardo SJ. Evaluation of a cathepsin-cleavable peptide linked radioimmunoconjugate of a panadenocarcinoma MAb, m170, in mice and patients. *Cancer Biother Radiopharm* 2004; **19:** 85-92.
27. Barrett AJ, Kirschke H. Cathepsin B, Cathepsin H, and cathepsin L. *Methods Enzymol* 1981; **80 Pt C:** 535-561.
28. Aronson NN, Jr., Barrett AJ. The specificity of cathepsin B. Hydrolysis of glucagon at the C-terminus by a peptidyldipeptidase mechanism. *Biochem J* 1978; **171:** 759-765.
29. Maciewicz RA, Etherington DJ, Kos J, Turk V. Collagenolytic cathepsins of rabbit spleen: a kinetic analysis of collagen degradation and inhibition by chicken cystatin. *Coll Relat Res* 1987; **7:** 295-304.
30. Mason RW. Interaction of lysosomal cysteine proteinases with alpha 2-macroglobulin: conclusive evidence for the endopeptidase activities of cathepsins B and H. *Arch Biochem Biophys* 1989; **273:** 367-374.
31. Gocheva V, Joyce JA. Cysteine cathepsins and the cutting edge of cancer invasion. *Cell Cycle* 2007; **6:** 60-64.
32. Wu C, Orozco C, Boyer J, Leglise M, Goodale J, Batalov S *et al*. BioGPS: an extensible and customizable portal for querying and organizing gene annotation resources. *Genome Biol* 2009; **10:** R130.
33. Su AI, Wiltshire T, Batalov S, Lapp H, Ching KA, Block D *et al*. A gene atlas of the mouse and human protein-encoding transcriptomes. *Proc Natl Acad Sci U S A* 2004; **101:** 6062-6067.
34. Su AI, Welsh JB, Sapinoso LM, Kern SG, Dimitrov P, Lapp H *et al*. Molecular classification of human carcinomas by use of gene expression signatures. *Cancer Res* 2001; **61:** 7388-7393.
35. Pesonen S, Kangasniemi L, Hemminki A. Oncolytic adenoviruses for the treatment of human cancer: focus on translational and clinical data. *Mol Pharm* 2011; **8:** 12-28.
36. Yan W, Kitzes G, Dormishian F, Hawkins L, Sampson-Johannes A, Watanabe J *et al*. Developing novel oncolytic adenoviruses through bioselection. *J Virol* 2003; **77:** 2640-2650.
37. Gros A, Martinez-Quintanilla J, Puig C, Guedan S, Mollevi DG, Alemany R *et al*. Bioselection of a gain of function mutation that enhances adenovirus 5 release and improves its antitumoral potency. *Cancer Res* 2008; **68:** 8928-8937.
38. Kuhn I, Harden P, Bauzon M, Chartier C, Nye J, Thorne S *et al*. Directed evolution generates a novel oncolytic virus for the treatment of colon cancer. *PLoS One* 2008; **3:** e2409.
39. Uil TG, Vellinga J, de Vrij J, van den Hengel SK, Rabelink MJ, Cramer SJ *et al*. Directed adenovirus evolution using engineered mutator viral polymerases. *Nucleic Acids Res* 2010.
40. Fallaux FJ, Kranenburg O, Cramer SJ, Houweling A, Van Ormondt H, Hoeben RC *et al*. Characterization of 911: a new helper cell line for the titration and propagation of early region 1-deleted adenoviral vectors. *Hum Gene Ther* 1996; **7:** 215-222.
41. Vellinga J, Uil TG, de Vrij J, Rabelink MJ, Lindholm L, Hoeben RC. A system for efficient generation of adenovirus protein IX-producing helper cell lines. *J Gene Med* 2006; **8:** 147-154.
42. de Vrij J, van den Hengel SK, Uil TG, Koppers-Lalic D, Dautzenberg IJ, Stassen OM *et al*. Enhanced transduction of CAR-negative cells by protein IX-gene

deleted adenovirus 5 vectors. *Virology* 2010.

43. Murakami P, McCaman MT. Quantitation of adenovirus DNA and virus particles with the PicoGreen fluorescent Dye. *Anal Biochem* 1999; **274:** 283-288.
44. Caravokyri C, Leppard KN. Constitutive episomal expression of polypeptide IX (pIX) in a 293-based cell line complements the deficiency of pIX mutant adenovirus type 5. *J Virol* 1995; **69:** 6627-6633.
45. DeNardo GL, DeNardo SJ, Peterson JJ, Miers LA, Lam KS, Hartmann-Siantar C *et al*. Preclinical evaluation of cathepsin-degradable peptide linkers for radioimmunoconjugates. *Clin Cancer Res* 2003; **9:** 3865S-3872S.
46. Uil TG, de Vrij J, Vellinga J, Rabelink MJ, Cramer SJ, Chan OY *et al*. A lentiviral vector-based adenovirus fiber-pseudotyping approach for expedited functional assessment of candidate retargeted fibers. *J Gene Med* 2009; **11:** 990-1004.
47. Douglas JT, Rogers BE, Rosenfeld ME, Michael SI, Feng M, Curiel DT. Targeted gene delivery by tropism-modified adenoviral vectors. *Nat Biotechnol* 1996; **14:** 1574-1578.
48. Durupt F, Koppers-Lalic D, Balme B, Budel L, Terrier O, Lina B *et al*. The chicken chorioallantoic membrane tumor assay as model for qualitative testing of oncolytic adenoviruses. *Cancer Gene Ther* 2011; doi:10.1038/cgt.2011.68.